

The progressive development of inhomogeneous shear and crystallographic fabric in glacial ice

PETER J. HUDLESTON

Department of Geology and Geophysics, University of Minnesota, Minneapolis, MN 55455, U.S.A.

(Received 17 May 1979; accepted in revised form 10 August 1979)

Abstract—Zones of shear, a few centimeters thick, in otherwise weakly deformed superimposed ice at the margin of the Barnes Ice Cap, are marked by decrease in plunge of elongate air bubbles, increase in degree of preferred crystallographic orientation, increase in grain size, and the development of a weakly sutured texture. The shear zone boundaries are parallel to bedrock and a direction of maximum shearing strain rate. In the interiors, shear strain attains values exceeding $\gamma = 10$, and the *c*-axes are tightly grouped in a cluster normal to the shear zone boundaries. With increase in overall deformation, the ice attains a high and apparently uniform shear strain by growth and coalescence of shear zones, leaving relict lenses of lower strain, or 'less-deformed zones', with characters opposite to those of the shear zones themselves.

INTRODUCTION

GLACIERS display a wide variety of structures varying from brittle fractures to strongly developed foliations and folds; all are formed in thin tongues or sheets of ice by the action of 'gravity tectonics'. Our relatively thorough understanding of the mechanics and kinematics of glacier flow provides a good framework for the interpretation of these structures (e.g. Hambrey 1977, Hambrey & Milnes 1977, Hudleston 1976, Hooke & Hudleston 1978).

Interesting observations on the development of inhomogeneous shear strain and preferred crystallographic orientations in ice can be made at the margin of the Barnes Ice Cap, Baffin Island, N.W.T., Canada. Details of the changes in texture and crystallographic fabric across one small shear zone in this ice cap have previously been described (Hudleston 1977), and it has been shown that there is similarity between individual shear zones found in ice and those developed in massive crystalline rocks (e.g. Ramsay & Graham 1970).

Additional observations on the shear zones in the Barnes Ice Cap are made in this paper, and progressive changes in the ice mass containing the shear zones are also considered. It will be shown that discrete shear zones are only evident at low to intermediate stages of deformation of the ice mass, and that at more intense average strains, typical of much of the marginal ice, the bulk of the ice acquires the characteristics of a single large shear zone. Relict pods of weakly deformed ice, referred to herein as 'less-deformed zones' are however locally preserved in the highly strained ice.

INITIAL STATE OF ICE AND TECTONIC SETTING

That part of the glacier in which the shear zones develop is made up of superimposed ice. This ice is formed by refreezing of meltwater that percolates into a wedge of wind-drift snow at the margin of the ice cap. It

initially consists of equant polygonal grains and contains numerous bubbles of roughly spherical shape (Fig. 1a & b). It displays either no preferred crystallographic orientation or a very weak, roughly vertical concentration of *c*-axes (Fig. 1c). A stratification parallel to the glacier surface (which dips down-glacier at about 10°) is marked by variations in grain size and bubble concentration.

During an advance of the glacier, the superimposed ice becomes overridden and deformed (Hooke 1973, Fig. 1, 1976, Fig. 3). Much of the glacier undergoes simple shear (Hudleston & Hooke in press), but near the margin simple shear is restricted to the basal ice. There is an overall longitudinal shortening component and vertical extensional component of strain rate in the marginal zone, and this increasingly modifies the shear component towards the surface. Flow is essentially isochoric and two-dimensional in this section of the glacier.

Both strain rate and cumulative deformation show an overall increase with depth and with distance up glacier, and this fact allows the effects of progressive deformation to be traced.

GEOMETRY AND TEXTURE OF SHEAR ZONES

The deformation produced in the overridden superimposed ice is quite inhomogeneous, and is characterized by the development of thin, ductile zones of shear, outlined by sigmoidal patterns of elongate air bubbles. Inclination of the bubbles is least at the centres of the zones (Fig. 2). Shear zones are found near the base of the glacier at the margin, and occur progressively higher above the bed up-glacier. Related structures, here referred to as 'less-deformed zones', appear below ice containing the shear zones (Fig. 3). The sigmoidal pattern is reversed in the less-deformed zones, with bubble inclination highest at the centres of the zones. The boundaries of both shear zones and less-deformed zones are sub-parallel to one another, the base of the

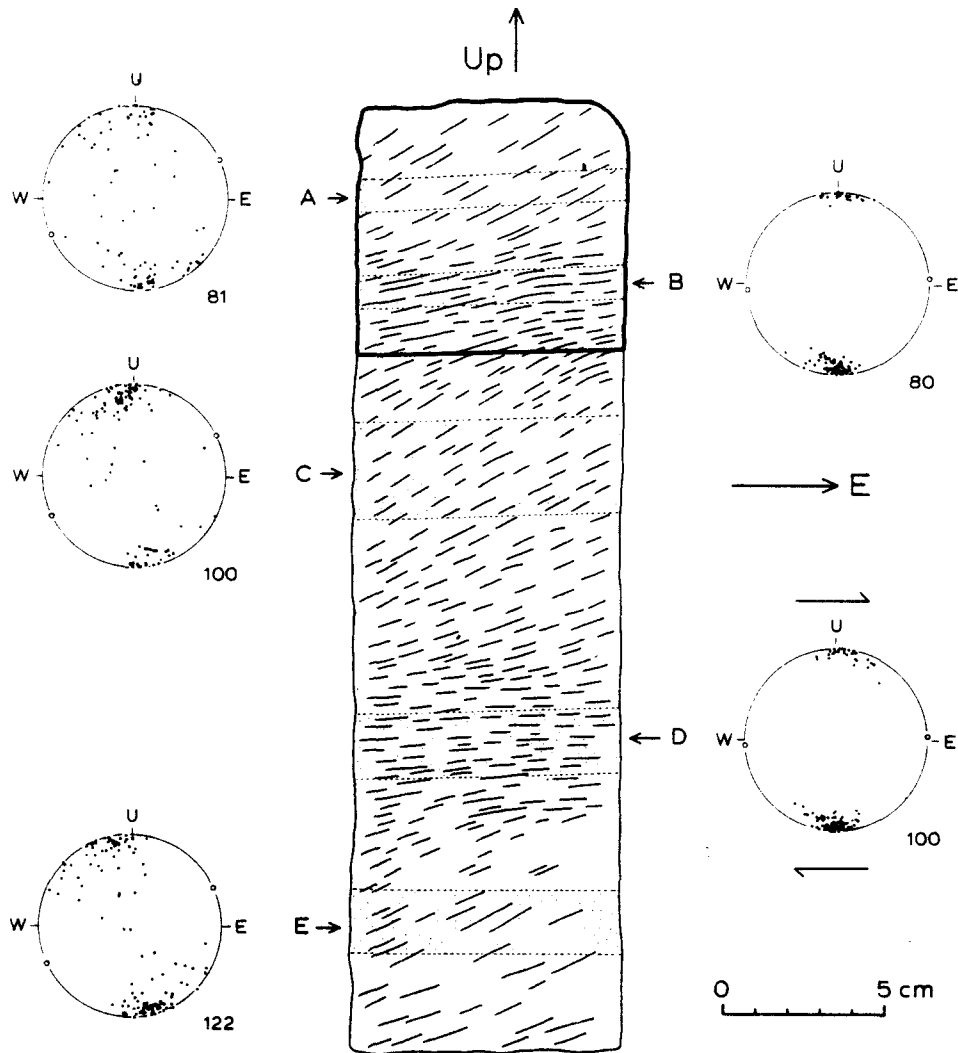


Fig. 2. Accurate tracing of bubbles in vertical slab (from middle of left shaft shown in Fig. 3) containing two shear zones. c-axis fabric data are for the stippled areas shown. The number of c-axes is given beside each plot; U is up; the large circle is the bubble trace. All equal-area lower hemisphere projections. The location of Fig. 4 is outlined with a heavy line.

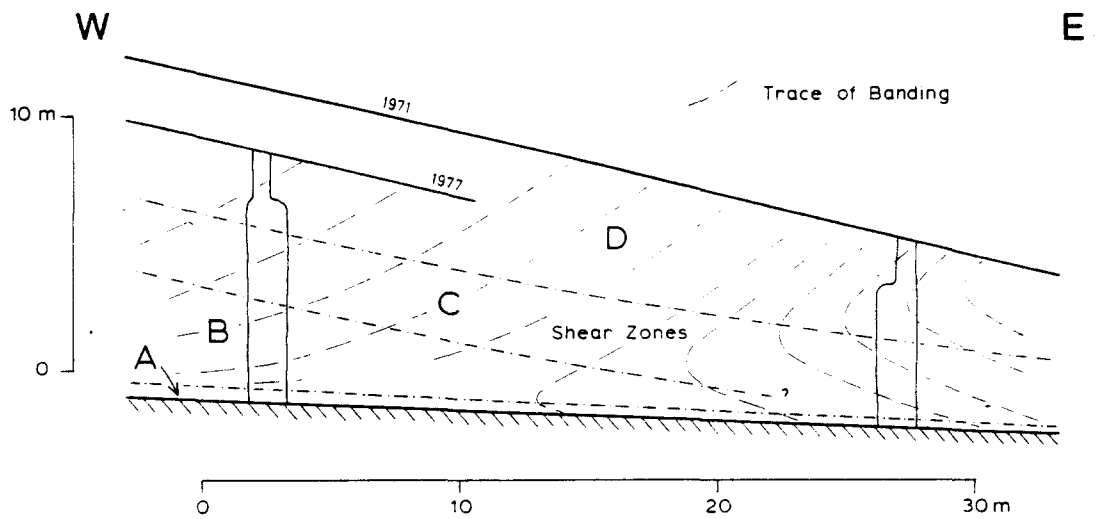


Fig. 3. Section of ice cap margin in the flow direction, with positions of glacier surface and observational shafts shown. Regions A-D indicate nature of bubble plunge. (A) Uniform and low plunge; (B) generally low plunge, but locally variable due to less-deformed zones; (C) generally moderate plunge, but variable due to shear zones; (D) uniform and high plunge.

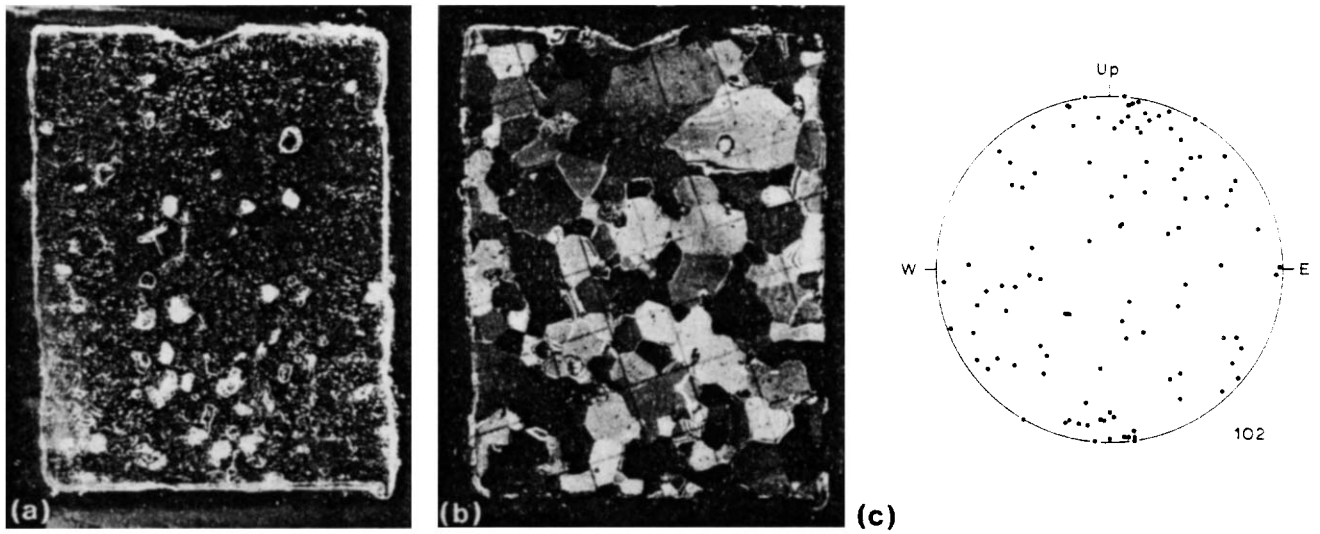


Fig. 1. (a) Vertical section (0.5 cm thick) of undeformed superimposed ice, showing included air bubbles. (b) Thin section of same slab under crossed polarizers to show grain texture. (c) Equal-area stereographic projection of 102 *c*-axes measured in the thin section. A centimeter grid is superimposed in b for scale.

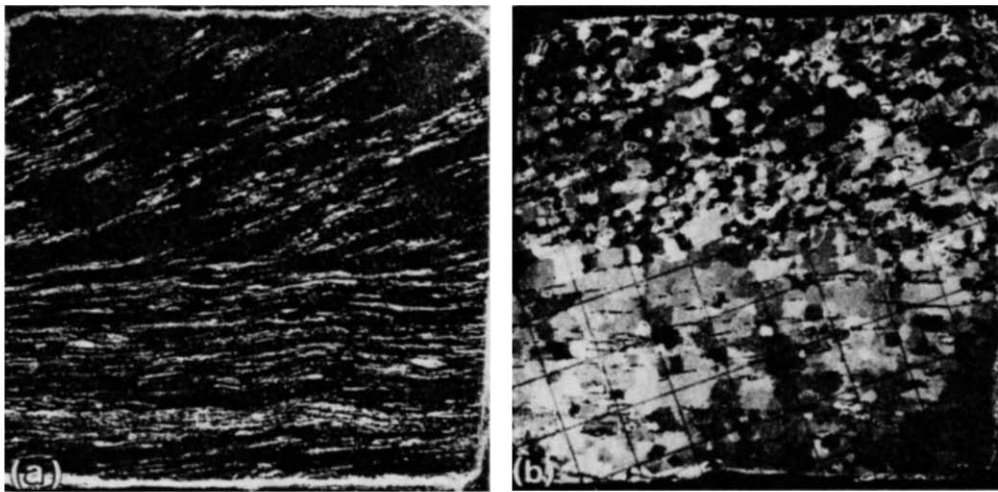


Fig. 4(a). Thick section (0.3 cm thick) and (b) thin section (under crossed polarizers) of upper part of slab shown in Fig. 2, showing bubble traces and grain textures across a shear zone boundary. Centimeter grid in (b) gives the scale.



glacier and to the measured direction of maximum shearing strain rate. The sense of displacement corresponds to the direction of ice flow. Individual zones are up to 1 m in length and 3 cm in thickness, with typical aspect ratios of about 20:1 for shear zones, and somewhat less for the less-deformed zones. It should be noted, however, that the sampled population is small and the dimensions difficult to measure because the shear zones grade laterally and longitudinally into the surrounding ice. No estimates of dimensions perpendicular to the flow direction could be made. Neither type of shear zone structure appears to be regularly spaced.

Textural changes across both shear zones and less-deformed zones are similar, but of opposite sense. The changes are summarized with reference to an example from region C of Fig. 3 and, for this example, the traces of elongate bubbles in a vertical slab of ice transected by two shear zones are shown in Fig. 2. Towards the centre of a shear zone there is an increase in grain size and the development of less regular and somewhat sutured shapes (Fig. 4). Grain shapes remain fairly equant throughout, with a slight tendency towards elongation parallel with the shear zone boundaries in the centres of the zones (Fig. 4). The most marked textural change is in the degree of preferred *c*-axis orientation, which increases from a weak or moderate fabric outside a shear zone to a very strong single maximum fabric near the centre (Fig. 2). The pattern is just the opposite for the less-deformed zones. There is some evidence that a double maximum fabric, of the kind observed in experimental simple shear tests (Kamb 1972), forms an intermediate stage between the rather diffuse fabrics found in the most weakly deformed ice (not seen in Fig. 2, but displayed by rows I and II in fig. 5 of Hudleston 1977) and the strong single maximum fabric. This is illustrated by fabric diagrams for A and E in Fig. 2. Found in the less pronounced fabric patterns but not in the experimental data is a scattering of *c*-axes across the diameter of the plot between the main concentrations of points (best shown in fabric plot for E in Fig. 2), to form a weak girdle or perhaps a crossed girdle.

The single maximum of *c*-axes, or the strongest of two maxima, is roughly perpendicular to the shear zone boundaries, reflecting the fact that most ice grains become better aligned for glide on the basal plane as the shear strain increases. A useful way of interpreting the *c*-axis fabric data is by considering deformation within individual grains, in which glide is restricted to a single slip system {0001}, and rotation of grains occurs so that they fit together in some optimal fashion. A simplified model of such deformation under bulk simple shear has been proposed by Etchecopar (1977), and the preferred orientations predicted by his model (Etchecopar 1977, Fig. 12) are remarkably similar to those observed in shear zones in ice (Fig. 2 and Hudleston 1977, Fig. 5), by nature of the presence and relative strength of two maxima, and their position relative to the shear plane. Also the direction of maximum bulk cumulative extension roughly bisects the two maxima and the second maximum tends to disappear at high strains, in both

model and ice fabrics. The transient maximum in Etchecopar's model represents grains in which slip is initially in the opposite sense to that of the overall shear: these grains tend to become locked in a position of low resolved shear stress in their slip plane. In the model, 'fracturing' of the grains allows them to become unlocked and to continue to deform and rotate. Recrystallization and grain boundary movement would help unlock ice grains, and would also provide the necessary adjustments between grains, which must develop overlaps and gaps in Etchecopar's model because only one slip system operates. Considering the complicating effects of recrystallization in ice and the simplifications of the model, the close correspondence between model and observed fabrics is perhaps surprising.

A more general computer-simulated model of fabric development by intracrystalline glide on several slip systems has been developed by Lister *et al.* (1978), and the fabric patterns displayed by ice in the shear zones are very similar to some natural and simulated patterns of *c*-axes in quartzites that have undergone simple shear where basal glide is dominant (Lister & Price 1978).

The degree of concentration of *c*-axes increases as the bubble plunge decreases, in a systematic manner as reported previously (Hudleston 1977). Data from additional shear zones and less-deformed zones are all consistent with the original data (Fig. 5).

I have previously argued (Hudleston 1977), and tacitly assumed above, that elongate bubbles in the ice give some indication of the amount of strain undergone (compare Figs. 1 and 4). Specifically, for simple shear, the angle between the long axes of the bubbles and the shear zone boundaries may be related to the amount of shear strain, γ , (if certain plausible assumptions about bubble behaviour are made, Hudleston 1977, Fig. 14). Where a bubbly layer has been offset across a shear

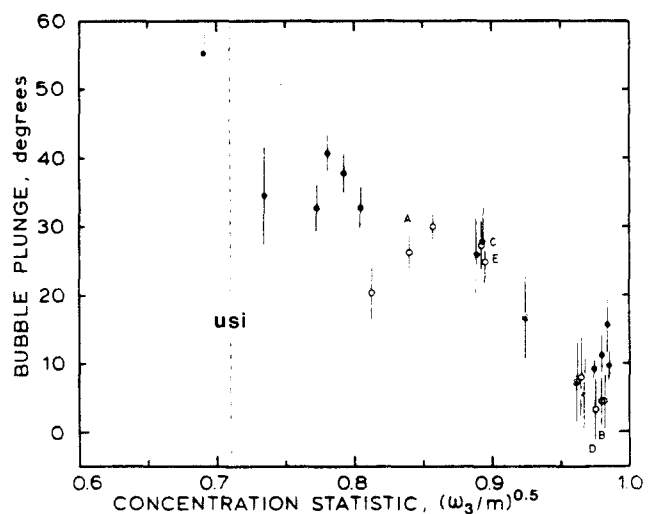


Fig. 5. Bubble plunge plotted against fabric intensity for shear zone data. Definitions and details are given in Bingham (1964) and Hudleston (1977). $(\omega_3/m)^{1/2}$ has a value of 1.0 for perfect point concentration and 0.58 for random distribution. Solid circles are data from Hudleston (1977); open circles are data for specimen shown in Fig. 2, with letters indicating locations; stars in circles are data for a less deformed zone (not illustrated). Error bars: one standard deviation from mean plunge. USI—data for undeformed superimposed ice of Fig. 1.

zone, a comparison of measured displacement with displacement predicted by the preferred model of bubble behaviour (Hudleston 1977, Fig. 14, curve a) produces good agreement. This provides support for using bubble orientation as a quantitative indicator of shear strain.

Applying this technique to the deformed superimposed ice containing shear zones and less deformed zones, values of γ ranging between less than 1 to much greater than 10 are obtained. For instance, estimates of γ of between 1 and about 10 have been made for the slab of ice shown in Fig. 2. It should be noted, however, that for $\gamma > 10$, large changes in γ are accompanied by very small changes in bubble inclination such that estimation errors become correspondingly large.

RELATIONS AMONG SHEAR ZONES, AND PROGRESSIVE DEFORMATION

In an earlier study (Hudleston 1977) and in the preceding sections of this paper, deformation has been considered as being due to simple shear alone. However, this cannot in general be the case, although it appears to be a good approximation in the best developed shear zones. If deformation is two-dimensional, isochoric, and in the form of planar bands (with no strain-variation along the bands), it must be in the form of differential simple shear with or without an additional homogeneous strain (as implied in Ramsay & Graham 1970, for example, where the unit matrix in equation 34 is replaced by a matrix of constants). These conditions are met closely for the central parts of shear zones with high aspect ratios. Also, for shear zones in the basal ice, which is frozen to the bed, there can be essentially no component of an homogeneous strain. This was the case for the shear zone previously described (Hudleston 1977).

Higher in the ice, the effects of a horizontal shortening and vertical extensional strain, superimposed on the shear strain, become significant. This explains why the stretched bubbles locally make angles of $>45^\circ$ with the shear zone boundaries (see Coward 1976, Fig. 3). In the upper ice we could consider the strain in the vicinity of a shear zone as the sum of a differential simple shear and an additional pure shear. To find the relative amounts of simple shear and pure shear, it would be necessary to measure both magnitude and orientation of strain (Coward 1976). This cannot be done here because bubble shapes are unreliable indicators of strain magnitude (Hudleston 1977). The shear zones displayed in Fig. 2 occur in the middle of the left-hand shaft shown in Fig. 3. It is not known how much pure shear is superimposed here, but its effect would be to increase both the value of γ and the strain ratio associated with a given bubble orientation. Such an effect is likely to be slight.

An additional reason for a departure from simple shear arises from the fact that the shear zones are of limited extent, and of approximately lensoid form. Coward (1976) has discussed the significance of a lensoid geometry on the deformation, and he pointed out

that compensatory 'flattening' strains near the ends of the shear zones are required to accommodate simple shear at their centres. Because shear zones almost certainly propagate along their length (Cobbold 1977a), simple shear will become superimposed on these end-related strains. The effect of such strains may not be great in the centres of the best-developed shear zones, but elsewhere the pattern of bubble elongation (Fig. 6) shows the kind of complication described by Coward (1976) for deformed dykes which show a complex network of shear zones. In Fig. 6 there is an overall parallelism of isogons of bubble plunge (as required for simple shear), but there is also a good deal of local deviation from this. There is at least one well-defined shear zone in Fig. 6, and several weak ones and incipient ones. The net effect is a complicated local strain pattern, although the region might still reasonably be treated in terms of an average simple shear (Cobbold 1977b).

The general disposition of shear zones and less deformed zones (Fig. 3) suggests an interesting history of progressive deformation. Because both strain rate and cumulative deformation increase on average with depth and with distance up-glacier, it appears that ice containing shear zones in region C (Fig. 3) will eventually become like ice in region B, both uniformly and highly strained, with the less-deformed zones representing local pockets of residual low strain.

Most shear zones develop in relatively homogeneous and isotropic ice (Fig. 1) by strain softening, involving intracrystalline glide, rotation and recrystallization of grains which become progressively better aligned for basal glide, thus weakening the aggregate of grains. Some shear zones probably develop in initially heterogeneous ice, for instance in a weaker bubbly layer, or in ice with a significant initial preferred orientation of *c*-axes. Strain softening will further weaken these as deformation progresses.

The shear zones form where the overall deformation pattern is one of simple shear. The fact that the velocity field departs progressively upwards from that required for simple shear may account for the lack of shear zones in the upper part of the ice (Fig. 3). With further overall deformation, the shear zones coalesce to form a mass of highly deformed ice, except for the less-deformed zones. How far the latter persist up glacier with increasing deformation is not known. The junction between highly deformed ice (with less-deformed zones) and more weakly deformed ice with shear zones is quite abrupt in the one place observed, so it is difficult to trace the details of the transition, and thus to know what the relative importance of lateral and longitudinal growth of old shear zones is to nucleation of new ones. It would appear, however, that to bring most of the ice to a state of uniformly high strain requires strain hardening to distribute the strain and prevent continued enhancement of the first-formed shear zones. It is possible that fairly large differences in strain are preserved in the highly deformed ice, but that these are masked because bubble elongation varies only slightly for large variations in shear strain where $\gamma > 10$. Even if such differ-

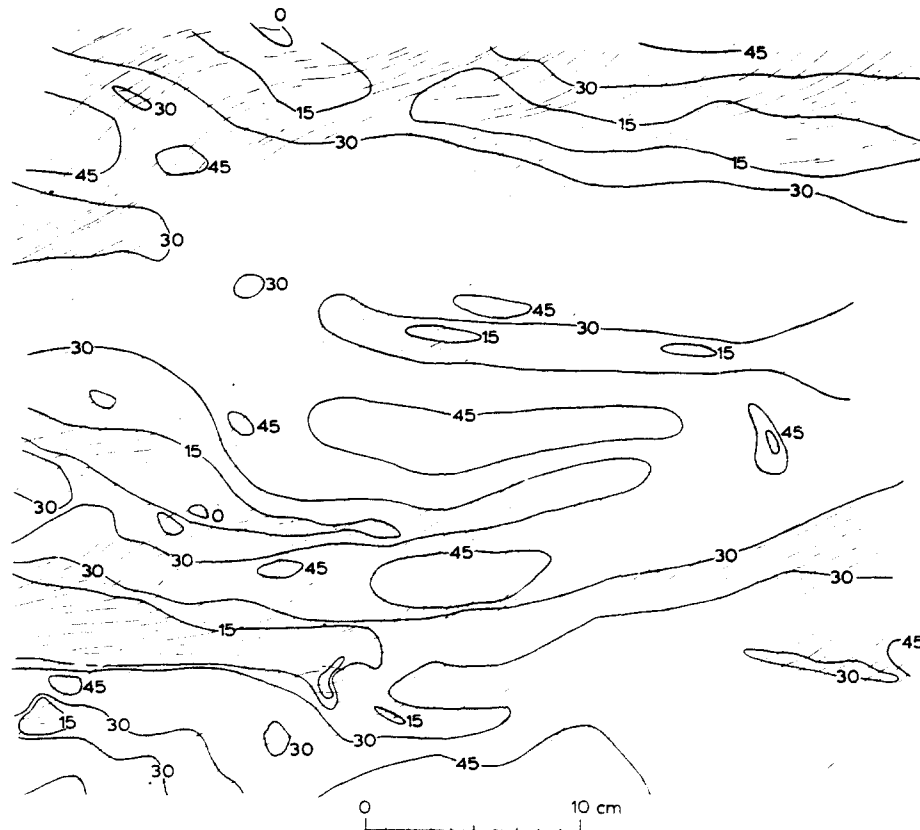


Fig. 6. Bubble traces and isogons of bubble plunge (contoured in degrees) for part of vertical wall, 1.5 m above the base, of right hand shaft shown in Fig. 3.

ences existed, some strain hardening would still be required. It is not clear what causes the strain hardening. The stress distribution around and within an ellipsoidal lens of weak material must, however, control the growth of the shear zone, and there must be a geometrical constraint on the amount of possible displacement, and hence internal shear, on a zone of given dimensions.

CONCLUSIONS

Characteristic textural changes are associated with the development of shear zones in the margin of the Barnes Ice Cap. Towards the interiors of shear zones, there is a decrease in bubble plunge, increase in grain size, increase in the degree of preferred *c*-axis orientation, and the development of sutured texture. Bubble orientation suggests shear strain, γ , varies between less than 1 to greater than 10 from least to most deformed ice.

Shear zones develop as local lensoid features in ice which has undergone a moderate average deformation of simple shear type. Local strain variations may be complicated and depart significantly from simple shear. As the average deformation increases, there is a transition to ice which is essentially one large shear zone, with locally preserved patches of low deformation, or less-deformed zones. Shear zones may thus represent a 'temporary' structure in ice that will eventually develop a high and apparently uniform strain. The mode of growth

and expansion of the shear zones is not clear, but presumably involves early strain softening and later strain hardening (cf. Cobbold 1977a).

Acknowledgements—This research was supported financially by the National Science Foundation (Grants GA-42728 & EAR-77-12990) and logistically by the Glaciology Division, Environment, Canada. The manuscript has been significantly improved by the comments and suggestions of Stan White and an anonymous reviewer.

REFERENCES

- Bingham C. 1972. An antipodally symmetric distribution on the sphere. *Ann. Stat.* **2**, 1201–1225.
- Cobbold, P. R. 1977a. Description and origin of banded deformation structures. II. Rheology and the growth of banded perturbations. *Can. J. Earth Sci.* **14**, 2510–2523.
- Cobbold, P. R. 1977b. Description and origin of banded deformation structures. I. Regional strain, local perturbations, and deformation bands. *Can. J. Earth Sci.* **14**, 1721–1731.
- Coward, M. P. 1976. Strain within ductile shear zones. *Tectonophysics* **34**, 181–197.
- Etchecopar, A. 1977. A plane kinematic model of progressive deformation in a polycrystalline aggregate. *Tectonophysics* **39**, 121–139.
- Hambrey, M. J. 1977. Foliation, minor folds and strain in glacier ice. *Tectonophysics* **39**, 397–416.
- Hambrey, M. J. & Milnes, A. G. 1977. Structural geology of an Alpine glacier (Griesgletscher, Valais, Switzerland). *Ecol. geol. Helv.* **70**, 667–684.
- Hooke, R. LeB. 1973. Flow near the margin of the Barnes Ice Cap, and the development of ice-cored moraines. *Bull. geol. Soc. Am.* **84**, 3929–3948.
- Hooke, R. LeB. 1976. Pleistocene ice at the base of the Barnes Ice Cap, Baffin Island, N.W.T., Canada. *J. Glaciol.* **17**, 49–60.

- Hooke, R. LeB. & Hudleston, P. J. 1978. Origin of foliation in glaciers. *J. Glaciol.* **20**, 285-299.
- Hudleston, P. J. 1976. Recumbent folding in the base of the Barnes Ice Cap, Baffin Island, Northwest Territories, Canada. *Bull. geol. Soc. Am* **87**, 1684-1692.
- Hudleston, P. J. 1977. Progressive deformation and development of fabric across zones of shear in glacier ice. In: *Energetics of Geological Processes* (edited by Saxena, S. & Bhattacharji, S.) Springer-Verlag, New York, 121-150.
- Hudleston, P. J. & Hooke, R. LeB. in press. Cumulative deformation in the Barnes Ice Cap and implications for the development of foliation. *Tectonophysics*.
- Kamb, B. 1972. Experimental recrystallization of ice under stress. In: *Flow and Fracture of Rocks* (edited by Heard, H. C., Borg, I. Y., Carter, N. L. & Raleigh, C. B.) *Am. Geophys. Union Monogr.* **16**, 210-241.
- Lister, G. S. & Price, G. P. 1978. Fabric development in a quartz-feldspar mylonite. *Tectonophysics* **49**, 37-78.
- Lister, G. S., Paterson, M. S. & Hobbs, B. E. 1978. The simulation of fabric development in plastic deformation and its application to quartzite: the model. *Tectonophysics* **45**, 107-158.
- Ramsay, J. G. & Graham, R. H. 1970. Strain variation in shear belts. *Can. J. Earth Sci.* **7**, 786-813.